Journal of Achievements in Materials and Manufacturing Engineering
VOLUME 37
ISSUE 2
December
2009

Structure and properties of selected Fe-based metallic glasses

R. Nowosielski, R. Babilas*
Division of Nanocrystalline and Functional Materials and Sustainable Pro-ecological Technologies, Institute of Engineering Materials and Biomaterials, Silesian University of Technology, ul. Konarskiego 18a, 44-100 Gliwice, Poland
* Corresponding author: E-mail address: rafal.babilas@polsl.pl

Received 12.10.2009; published in revised form 01.12.2009

Materials

ABSTRACT

Purpose: The paper presents a structure characterization, thermal and soft magnetic properties of Fe-based bulk amorphous materials in as-cast state and after crystallization process.
Design/methodology/approach: The studies were performed on $Fe_{72}B_{20}Si_4Nb_4$ metallic glass in form of ribbons and rods. The amorphous structure of tested samples was examined by X-ray diffraction (XRD), transmission electron microscopy (TEM) and scanning electron microscopy (SEM) methods. The thermal properties of the glassy samples were measured using differential thermal analysis (DTA) and differential scanning calorimetry (DSC). The soft magnetic properties examination of tested material contained magnetic permeability and magnetic after-effects measurements.
Findings: The X-ray diffraction and transmission electron microscopy investigations revealed that the studied as-cast materials were amorphous. Broad diffraction halo could be seen for all tested samples, indicating the formation of a glassy phase with the diameters up to 2 mm. The fracture surface of rod samples appears to consist of two different zones, which probably inform about different amorphous structures of studied glassy materials. A two stage crystallization process was observed for studied alloy. The first stage of crystallization corresponding to the partial crystallization of α-Fe phase was followed by the formation of iron borides. It has shown that appropriate increasing of annealing temperature, significantly improved soft magnetic properties of examined alloy.
Practical implications: The studied Fe-based metallic glass has good glass-forming ability and thermal stability for casting in form of ribbons and rods. The soft magnetic properties of studied alloy could be improved by applying the appropriate conditions of heat treatment (crystallization process).
Originality/value: The applied investigation methods are suitable to determine the changes of structure in function of sample thickness and the improvement of its magnetic properties after crystallization in comparison with as-cast state.
Keywords: Amorphous materials; Bulk metallic glasses; Soft magnetic properties; Crystallization

Reference to this paper should be given in the following way:
R. Nowosielski, R. Babilas, Structure and properties of selected Fe-based metallic glasses, Journal of Achievements in Materials and Manufacturing Engineering 37/2 (2009) 332-339.

1. Introduction

The Fe-based metallic glasses are studied as an interesting class of engineering materials, which have good soft magnetic properties. Those properties are attractive compared with conventional crystalline alloys and they are very useful in a wide range of technical applications [1].

It is generally known that preparation of glassy materials requires high critical cooling rates of about 10^6 K/s. However, Inoue et al. proposed some alloys, which have good glass-forming ability with good soft magnetic properties in the amorphous state [2,3]. These alloys could be prepared in different forms like ribbons, rods and rings with low critical cooling rates below 10^3 K/s [4].

Fe-based bulk metallic glasses with critical cooling rates below 10^3 K/s have been often found in Fe-based alloy systems containing metalloids (B, C, Si, and P) and early transition elements (Zr, Nb, Hf) [5].

Good glass-forming ability (GFA) of metallic alloys could be achieved by realizing empirical rules proposed by Inoue. These rules said that alloy with good GFA should consisting of more than three elements. The elements should have a difference in atomic size ratios above about 12% and negative heats of mixing. The first Fe-based bulk glassy alloys (realized Inoue's empirical rules) were prepared in 1995, since then, a variety of Fe-based bulk glassy alloys have been prepared [4].

This paper presents some results of $Fe_{72}B_{20}Si_4Nb_4$ alloy, which has good soft magnetic properties. Soft magnetic properties of Fe-based ferromagnetic metallic glasses could be significantly improved by a controlling heat treatment (relaxation and crystallization process) [6].

Crystallization process can be precisely investigated by many experimental methods like differential scanning calorimetry (DSC), X-ray diffraction (XRD) and transmission electron microscopy (TEM). These studies can also provide information for understanding the influence of microstructure changes under heat activation like structural relaxation, nanocrystallization and crystallization on physical properties [7].

2. Material and research methodology

The aim of the present work is the microstructure characterization, thermal and soft magnetic properties analysis of $Fe_{72}B_{20}Si_4Nb_4$ bulk amorphous alloy in as-cast state and after crystallization process. Investigations were done by using XRD, TEM, SEM, DTA, DSC and magnetic's measurement methods.

The investigated material was cast in form of ribbons with thickness of g = 0.03, 0.05, 0.06, 0.08, 0.15 and 0.20 mm and rods with diameter of ø = 1.5 and 2 mm (Fig.1).

The ribbons were manufactured by the "chill-block melt spinning" (CBMS) technique, which is a method of continuous casting of the liquid alloy on the surface of a turning copper based wheel [8-11]. The casting conditions include linear speed of copper wheel 20 m/s and ejection over-pressure of molten alloy: 0.02 MPa. Moreover, rods were manufactured by the pressure die casting. The pressure die casting technique [12,13] is a method of casting a molten alloy into copper mould under a protective gas pressure.

Fig. 1. Outer morphology of cast glassy $Fe_{72}B_{20}Si_4Nb_4$ alloy rods with diameters of 1.5 and 2 mm

The chemical composition of studied Fe-based metallic glass allows to cast this kind of material in bulk forms, but in this work used samples in form of ribbons and rods.

In order to study a crystallization processes, samples in the "as-cast" state were annealed at the temperature range from 373 K to 923 K with the step of 50 K. Tested ribbons were annealed in electric chamber furnace THERMOLYNE 6020C under protective argon atmosphere. The annealing time was constant and equaled to 1 hour.

Structure analysis of studied materials in as-cast state was carried out using Seifert-FPM XRD 7 diffractometer with $Co_{K\alpha}$ radiation for ribbon samples measurements and PANalytical X'Pert diffractometer with $Co_{K\alpha}$ radiation for rod samples examination.

Phase analysis of ribbon after crystallization process was carried out using the X-Pert Philips diffractometer equipped with curved graphite monochromator on diffracted beam and a tube provided with copper anode. It was supplied by current intensity of 30 mA and voltage of 40 kV. The length of radiation ($\lambda CuK\alpha$) was 1.54178 Å. The data of diffraction lines were recorded by "step-scanning" method in 2θ range from 30° to 90° and 0.05° step.

The fracture morphology of studied glassy material in form of rods with diameter of 1.5 and 2 mm was analyzed using the scanning electron microscopy (SEM) with magnification up to 1000x.

Transmission electron microscopy (TESLA BS 540) was used for the structural characterization of studied samples after annealing process. Thin foils for TEM observation were prepared by an electrolytic polishing method after a mechanical grinding.

The thermal properties associated with crystallization temperature of the amorphous ribbons were measured using the differential thermal analysis (Mettler - DTA) at a constant heating rate of 6 K/m under an argon protective atmosphere.

The differential scanning calorimetry (DSC, SDT Q600) was used to determine crystallization, glass transition temperature and Curie temperature for tested glassy alloy in form of rods. The heating rate of calorimetry measurements was 20 K/min.

Magnetic measurements of annealed samples (determined at room temperature) included following properties:

(1) relative magnetic permeability - determined by Maxwell-Wien bridge at a frequency of 1030 Hz and magnetic field

H= 0.5 A/m), (magnetic permeability measurements were carried out for samples of length of 100 mm);

(2) magnetic permeability relaxation $\Delta\mu/\mu$ (magnetic after-effects) - determined by measuring changes of magnetic permeability as a function of time after demagnetization, where $\Delta\mu$ is difference between magnetic permeability determined at t_1 = 30 s and t_2 = 1800 s after demagnetization and μ at t_1 [14,15].

3. Results and discussion

The X-ray diffraction investigations reveal that the studied as-cast glassy samples were amorphous. The diffraction patterns of tested ribbons with thickness from 0.03 mm to 0.20 mm (Fig.2) and rods with diameter of 1.5 and 2 mm (Fig.3) show the broad diffraction halo characteristic for the amorphous structure.

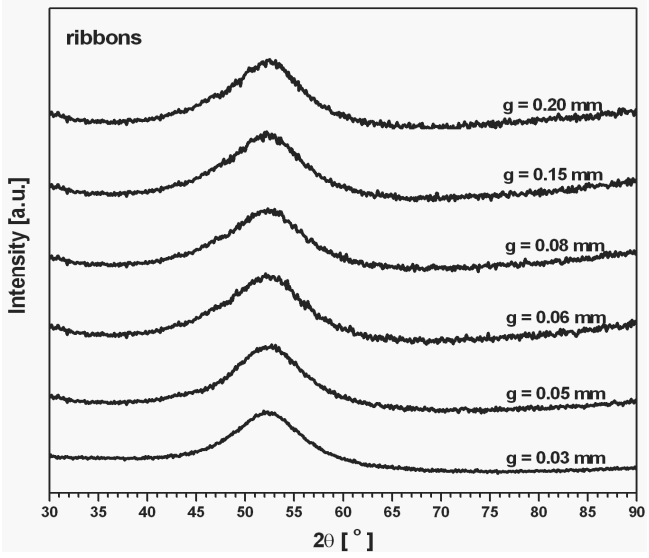

Fig. 2. X-ray diffraction patterns of $Fe_{72}B_{20}Si_4Nb_4$ glassy ribbons in as-cast state with thickness from 0.03 mm to 0.20 mm

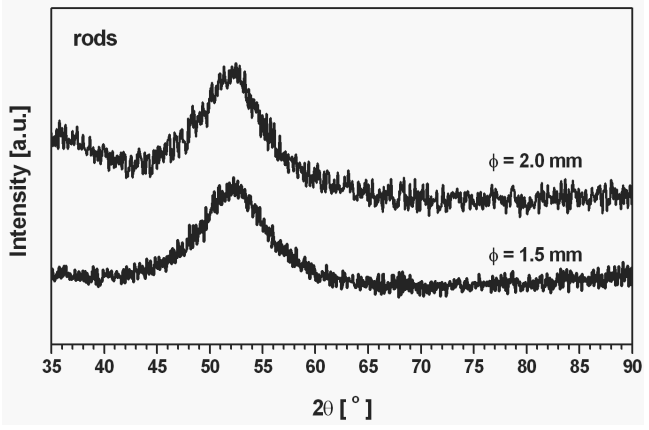

Fig. 3. X-ray diffraction patterns of $Fe_{72}B_{20}Si_4Nb_4$ glassy rods in as-cast state with diameter of 1.5 and 2 mm

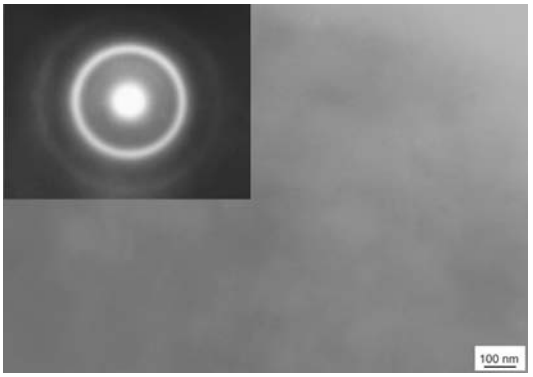

Fig. 4. Transmission electron micrograph and electron diffraction pattern of the as-cast glassy $Fe_{72}B_{20}Si_4Nb_4$ ribbon with a thickness of 0.03 mm

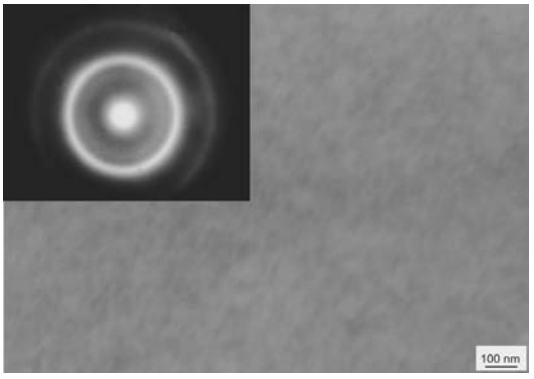

Fig. 5. Transmission electron micrograph and electron diffraction pattern of the as-cast glassy $Fe_{72}B_{20}Si_4Nb_4$ rod with a diameter of 1.5 mm

Figures 4 and 5 show TEM images and electron diffraction patterns of chosen samples in as-cast state: ribbon with thickness of 0.03 mm and rod with diameter of 1.5 mm, adequately.

The TEM images reveal only a changing of contrast and no appreciable contrast corresponding to a crystalline phase is seen. The electron diffraction pattern consists only of halo rings. Broad diffraction halo can be seen for all tested samples, indicating the formation of a glassy phase with the diameters up to 2 mm.

The DTA curves (at 6 K/min) measured on amorphous ribbons with thickness of 0.03, 0.08 and 0.20 mm in as-cast state for examined alloy are shown in Figure 6.

A two stage crystallization process was observed. The exothermic peaks describing crystallization effects are situated very near. The first stage crystallization of studied alloy for ribbon with thickness of 0.03 mm includes onset crystallization temperature (T_{x1} = 842 K) and peak crystallization temperature (T_{p1} = 864 K). Moreover, analysis of the second crystallization stage allows to determine only peak crystallization temperature (T_{p2} = 892 K), as well.

For ribbon with thickness of 0.08 mm the first stage of crystallization includes onset crystallization temperature at value of T_{x1} = 853 K and peak crystallization temperature at T_{p1} = 869 K. Analysis of the second crystallization stage of studied ribbon allows to determine peak crystallization temperature, which has a value of T_{p2} = 893 K, as well.

The DTA analysis of ribbon with thickness of 0.20 mm informs the first stage of crystallization includes onset crystallization temperature at value of T_{x1} = 857 K and peak crystallization temperature at T_{p1} = 871 K. The second crystallization stage of studied ribbon is determined by peak crystallization temperature, with a value of T_{p2} = 890 K, as well.

The analysis of crystallization process of examined ribbons shows that crystallization temperature's peak increase with increasing samples thickness during first stage of crystallization and decrease during second stage of crystallization. The differences of crystallization temperature between ribbons with different thickness of the same alloy are probably caused by different amorphous structures as a result of the different cooling rates of studied metallic glasses.

The DSC curves (at 20 K/min) measured on amorphous rods with diameter of 1.5 and 2 mm in as-cast state for studied alloy are shown in Figure 7. Results of DSC investigations for rods confirmed that crystallization temperature increase with increasing of sample diameter. It is another reason for changing the amorphous structure with sample thickness.

The DSC examinations of rod samples allow to determine the peak crystallization temperature: Tp1 = 884 K for sample with diameter of 1.5 mm and Tp1 = 885 K for sample with diameter of 2 mm. The glass transition temperature (Tg = 817 K for diameter of 1.5 mm, Tg = 825 K for diameter of 2 mm) was determined as well.

Moreover, the DSC results allow to determine Curie temperature (T_c) for studied glassy rods. The Curie temperature (T_c) of rod with diameter of 1.5 mm has a value of 567 K and for rod with diameter of 2 mm, T_c = 570 K (Fig.7). A variation of the Curie temperature is probably also due to different amorphous structures of the tested rods with increasing thickness.

The crystallization temperatures obtained from DTA and DSC curves are connected with thermal properties of studied bulk metallic glass in form of ribbons and rods in as-cast state.

The appearance of the fracture surface was investigated by SEM method at different magnifications. Figure 8 shows micrographs of as-cast glassy rod with diameter of 1.5 mm. What is more, Figures 9 and 10 present images of glassy rods with diameter of 2 mm, similarly.

The fracture surface appears to consist of small fracture zones, which leads to breaking of the samples into parts. The presented fractures could be classified as mixed fractures with indicated two zones contain "river" patterns (Zone I) and "smooth" areas (Zone II). The "river" patterns (marked as Zone I) are characteristic for metallic glassy alloys. The fracture surface of rod samples appears to consist of two different zones, which probably inform about different structures of studied glassy materials.

Figure 11 shows X-ray diffraction patterns obtained for studied alloy in form of ribbon after annealing at 823, 873 and 923 K for 1 hour.

Annealing at temperature above 823 K obviously causes formation of crystalline phases. Qualitative phase analysis from X-ray data enables the identification of α-Fe phase (823 K) and borides Fe_2B, Fe_3B and $Fe_{23}B_6$ (873 K and 923 K). Moreover, X-ray diffraction investigations allow to detection Nb_3Si.

The TEM examinations also confirmed a formation of crystalline phases in samples after annealing at temperatures higher than 823 K. Figures 12 and 13 present TEM micrograph, electron diffraction pattern and its solution for samples annealed at 873 K and 923 K, adequately.

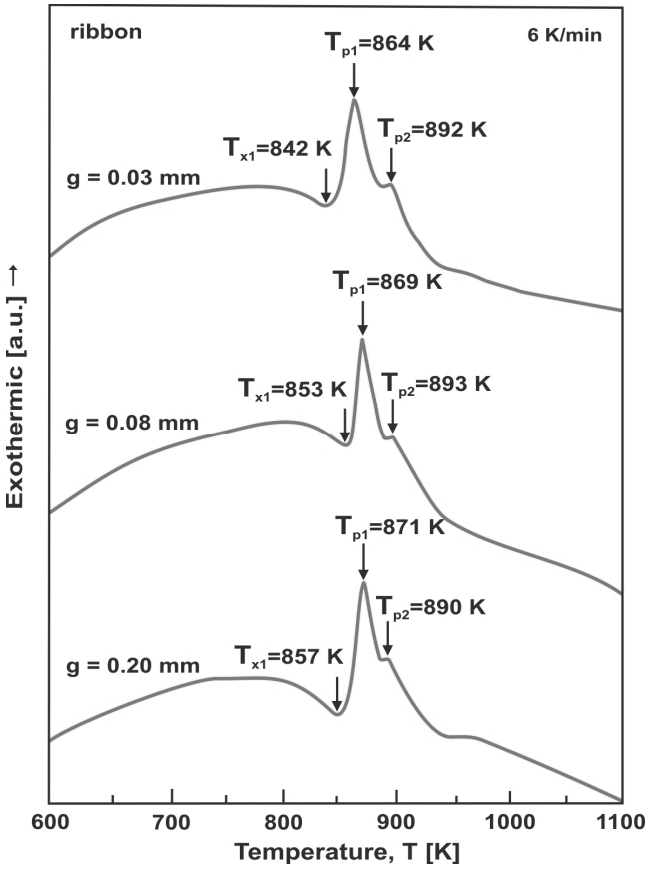

Fig. 6. DTA curves of $Fe_{72}B_{20}Si_4Nb_4$ glassy alloy ribbons in as-cast state (heating rate 6 K/min)

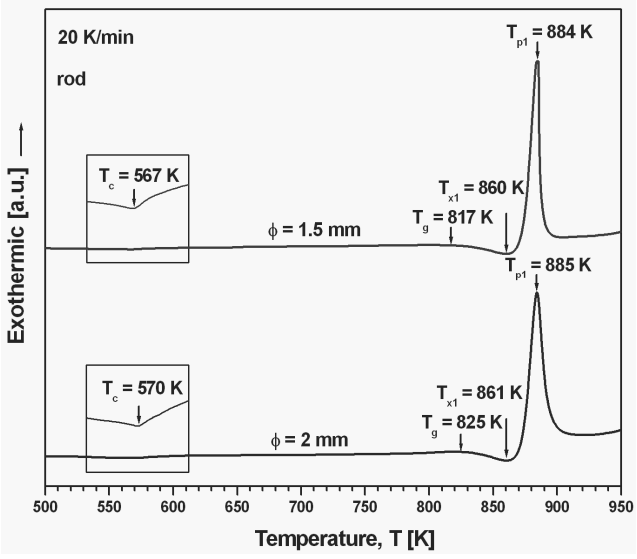

Fig. 7. DSC curves of $Fe_{72}B_{20}Si_4Nb_4$ glassy alloy rods in as-cast state (heating rate 20 K/min)

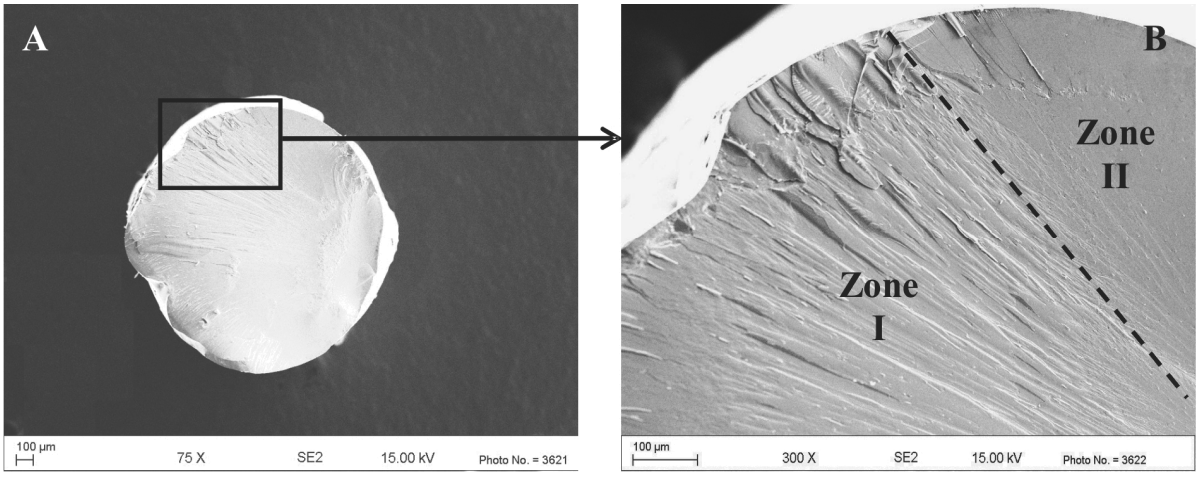

Fig. 8. SEM micrographs of the fracture morphology of $Fe_{72}B_{20}Si_4Nb_4$ amorphous rod in as-cast state with diameter of 1.5 mm: A – magn. 75x, B – magn. 300x

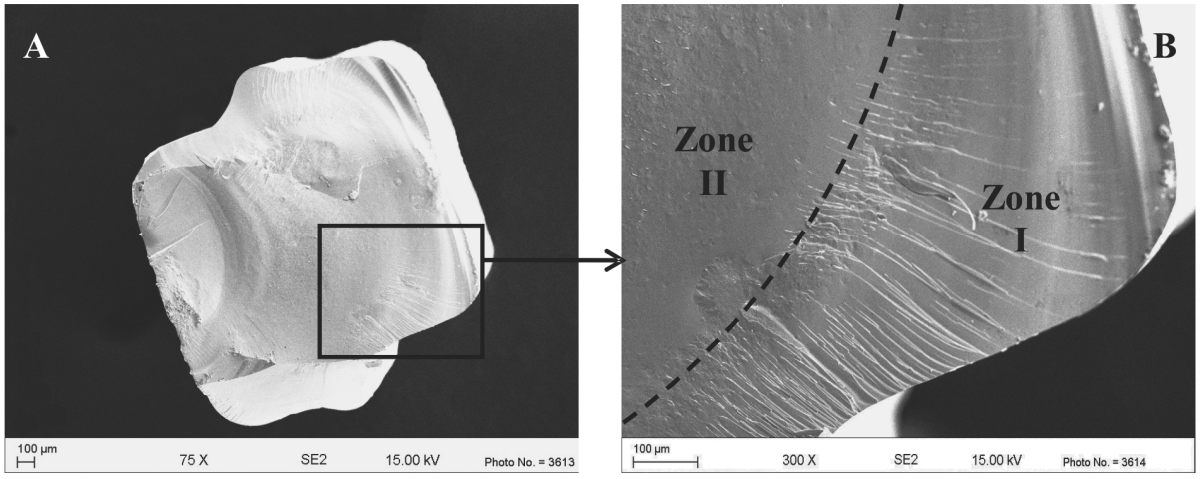

Fig. 9. SEM micrographs of the fracture morphology of $Fe_{72}B_{20}Si_4Nb_4$ amorphous rod in as-cast state with diameter of 2 mm: A – magn. 75x, B – magn. 300x

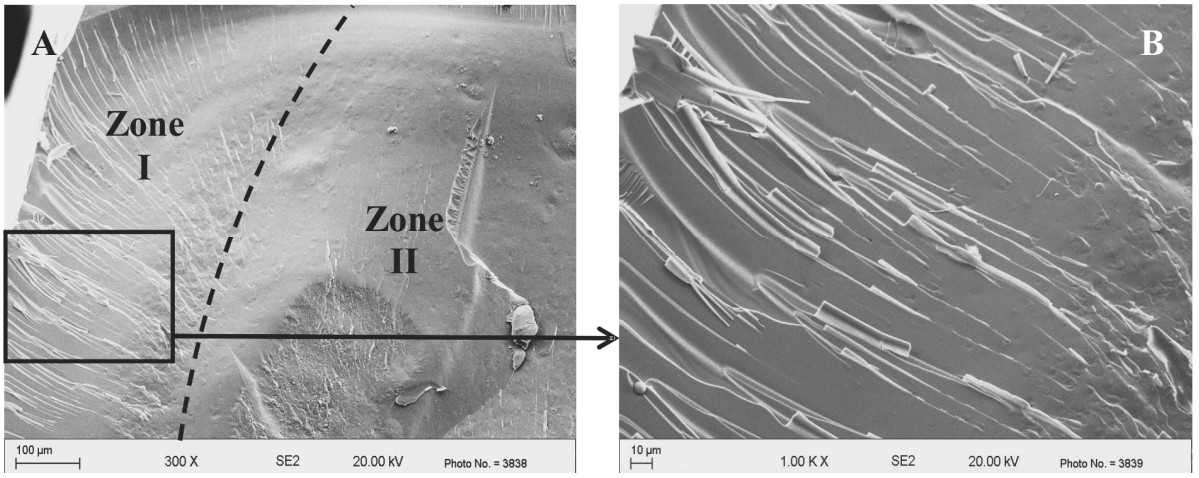

Fig. 10. SEM micrographs of the fracture morphology of $Fe_{72}B_{20}Si_4Nb_4$ amorphous rod in as-cast state with diameter of 2 mm: A – magn. 300x, B – magn. 1000x

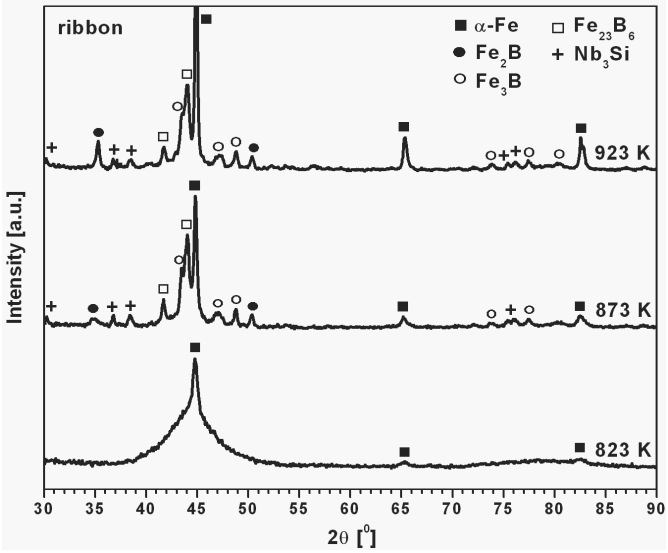

Fig. 11. X-ray diffraction patterns of $Fe_{72}B_{20}Si_4Nb_4$ alloy (ribbon) after annealing at 823, 873 and 923 K for 1 hour

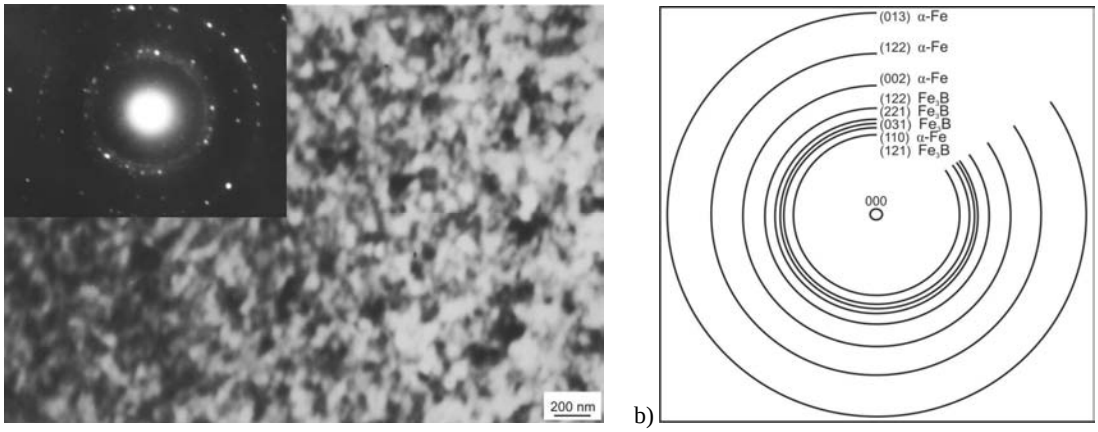

Fig. 12. Transmission electron micrograph plus electron diffraction pattern (a) and solution of diffraction pattern (b) of $Fe_{72}B_{20}Si_4Nb_4$ alloy in form of ribbon after annealing at 873 K for 1 hour

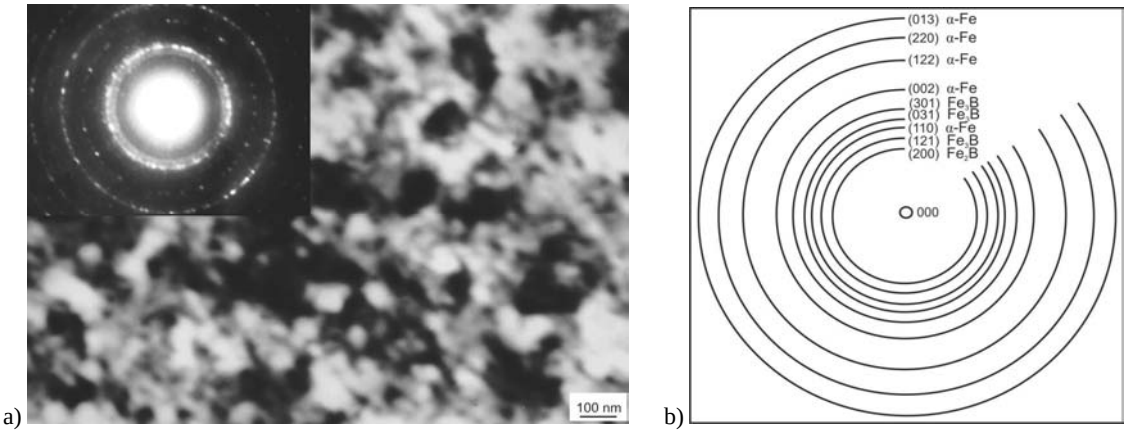

Fig. 13. Transmission electron micrograph plus electron diffraction pattern (a) and solution of diffraction pattern (b) of $Fe_{72}B_{20}Si_4Nb_4$ alloy in form of ribbon after annealing at 923 K for 1 hour

The initial magnetic permeability (μ_r) determined at room temperature versus annealing temperature (T_a) is shown in Fig.14. The initial magnetic permeability of examined alloy increases together with increasing of annealing temperature and reaches a distinct maximum at 773 K similarly for ribbon and rod samples. The temperature of annealing process, which corresponds to the maximum of initial magnetic permeability (μ_{rmax} = 2550 for ribbon, μ_{rmax} = 650 for rods) can be defined as the optimization annealing temperature (T_{op}).

However, distinct differences in the initial magnetic permeability between ribbons and rods could be explained by the different amorphous structure (higher cooling rates applied in the ribbons casting process).

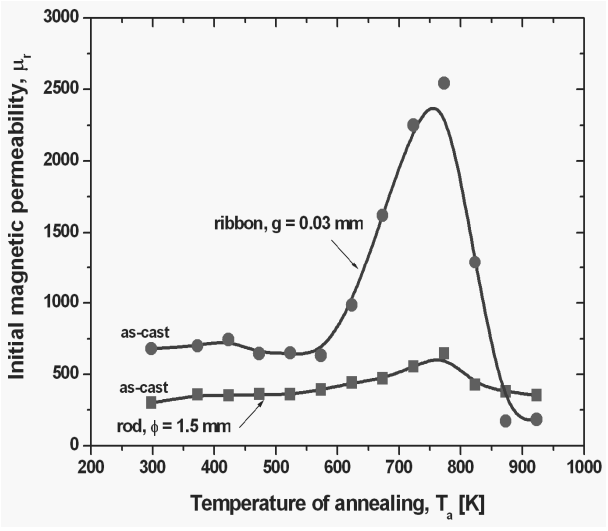

Fig. 14. Initial magnetic permeability of $Fe_{72}B_{20}Si_4Nb_4$ alloy determined at room temperature versus annealing temperature

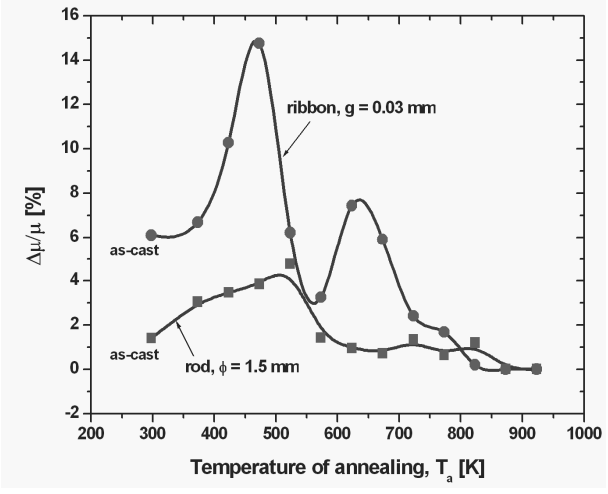

Fig. 15. Magnetic permeability relaxation of $Fe_{72}B_{20}Si_4Nb_4$ alloy determined at room temperature versus annealing temperature

Magnetic permeability relaxation (defined as magnetic after-effects) in function of annealing temperature is shown in Fig.15. The intensity of $\Delta\mu/\mu$ is directly proportional to the concentration of defects in amorphous materials, i.e. free volume concentration [1,14,15]. The value of $\Delta\mu/\mu$ increases in the temperature range from 373 K to 473 K and from 373 K to 523 K for ribbons and rods, respectively.

The successive increase of annealing temperature causes the decrease of $\Delta\mu/\mu$ at temperatures higher than 523 K for rods and 623 K for ribbons. It is significant that the optimization annealing temperature (T_{op}) corresponds to the decrease of magnetic instability ($\Delta\mu/\mu$). This means that the optimization annealing reduces time instabilities (free volume) of magnetic permeability.

Additionally, Figures 14 and 15 present values of μ_r and $\Delta\mu/\mu$ in as-cast state of examined ribbons and rods.

Table 2.
Magnetic properties of studied $Fe_{72}B_{20}Si_4Nb_4$ alloy at optimization annealing temperature (T_{op})

Sample	T_{op} [K]	μ_r	$\Delta\mu/\mu$ [%]
Ribbon (g = 0.03 mm)	773	2550	1.7
Rod (ø = 1.5 mm)	773	650	0.6

Table 2 also gives information about magnetic properties of studied alloy in from of ribbon (g = 0.03 mm) and rod (ø = 1.5 mm) after optimization annealing temperature (T_{op}).

4. Conclusions

The investigations performed on the samples of $Fe_{72}B_{20}Si_4Nb_4$ metallic glass in as-cast state and after crystallization process allowed to formulate the following statements:

- the X-ray diffraction and transmission electron microscopy investigations revealed that the studied as-cast bulk metallic glasses (ribbons and rods) were amorphous,
- the SEM images showed that studied fractures could be classified as mixed fractures with indicated two zones contained "river" and "smooth" areas,
- changes of Curie temperature, crystallization temperature and glass transition temperature as a function of glassy samples thickness (cooling rate) were stated,
- the annealing treatment caused a formation of crystalline phases (α-Fe and iron borides) at temperature above 823 K,
- the initial magnetic permeability increased together with the increase of annealing temperature and reached a distinct maximum at 773 K for ribbons and rods,
- optimized annealing temperature (T_{op}) is connected with significant decrease of magnetic instability ($\Delta\mu/\mu$),
- the optimization effect (a real improvement of the initial magnetic permeability) takes place in amorphous phase of studied alloy.

Acknowledgements

The authors would like to thank Dr A. Zajączkowski, Dr W. Głuchowski (Non-Ferrous Metals Institute, Gliwice), Dr Z. Stokłosa (Institute of Materials Science, University of Silesia, Katowice) and Dr T. Czeppe (Institute of Metallurgy and Materials Science, Kraków) for a cooperation and helpful comments.

This work is supported by Polish Ministry of Science (grant N507 027 31/0661).

References

[1] J. Rasek, Some diffusion phenomena in crystalline and amorphous metals, Silesian University Press, Katowice, 2000 (in Polish).
[2] A. Inoue, High strength bulk amorphous alloys with low critical cooling rates, Materials Transactions JIM 36 (1995) 866-875.
[3] A. Inoue, A. Makino, T. Mizushima, Ferromagnetic bulk glassy alloys, Journal of Magnetism and Magnetic Materials 215-216 (2000) 246-252.
[4] A. Inoue, Bulk amorphous and nanocrystalline alloys with high functional properties, Materials Science and Engineering A304-306 (2001) 1-10.
[5] A. Inoue, B.L. Shen, C.T. Chang, Fe- and Co-based bulk glassy alloys with ultrahigh strength of over 4000 MPa, Intermetallics 14 (2006) 936-944.
[6] R. Nowosielski, R. Babilas, S. Griner, G. Dercz, A. Hanc, Crystallization of $Fe_{72}B_{20}Si_4Nb_4$ metallic glasses ribbons, Journal of Achievements in Materials and Manufacturing Engineering 34/1 (2009) 15-22.
[7] T. Kulik, Nanocrystallization of metallic glasses, Journal of Non-Crystalline Solids, 287 (2001) 145-161.
[8] D. Szewieczek, J. Tyrlik-Held, S. Lesz, Structure and mechanical properties of amorphous $Fe_{84}Nb_7B_9$ alloy during crystallization, Journal of Achievements in Materials and Manufacturing Engineering 24/1 (2007) 87-90.
[9] D. Szewieczek, T. Raszka, J. Olszewski, Optimisation the magnetic properties of the $(Fe_{1-x}Co_x)_{73.5}Cu_1Nb_3Si_{13.5}B_9$ (x=10; 30; 40) alloys, Journal of Achievements in Materials and Manufacturing Engineering 20 (2007) 31-36.
[10] S. Lesz, D. Szewieczek, J.E. Frąckowiak, Structure and magnetic properties of amorphous and nanocrystalline $Fe_{85.4}Hf_{1.4}B_{13.2}$ alloy, Journal of Achievements in Materials and Manufacturing Engineering 19 (2006) 29-34.
[11] S. Lesz, D. Szewieczek, J. Tyrlik-Held, Correlation between fracture morphology and mechanical properties of NANOPERM alloys, Archives of Materials Science and Engineering 29/2 (2008) 73-80.
[12] R. Nowosielski, R. Babilas, Structure and magnetic properties of $Fe_{36}Co_{36}B_{19}Si_5Nb_4$ bulk metallic glasses, Journal of Achievements in Materials and Manufacturing Engineering 30/2 (2008) 135-140.
[13] R. Nowosielski, R. Babilas, S. Griner, Z. Stokłosa, Structure and soft magnetic properties of $Fe_{72}B_{20}Si_4Nb_4$ bulk metallic glasses, Archives of Materials Science and Engineering 35/1 (2009) 13-20.
[14] Z. Stokłosa, J. Rasek, P. Kwapuliński, G. Haneczok, G. Badura, J. Lelątko, Nanocrystallisation of amorphous alloys based on iron, Materials Science and Engineering C 23 (2003) 49-53.
[15] P. Kwapuliński, Z. Stokłosa, J. Rasek, G. Badura, G. Haneczok, L. Pająk, L. Lelątko, Influence of alloying additions and annealing time on magnetic properties in amorphous alloys based on iron, Journal of Magnetism and Magnetic Materials 320 (2008) 778-782.